Virus fate and transport during artificial recharge with recycled water

Robert Anders

U.S. Geological Survey, San Diego, California, USA

Department of Civil and Environmental Engineering, University of California, Irvine, California, USA

C. V. Chrysikopoulos

Department of Civil and Environmental Engineering, University of California, Irvine, California, USA

Department of Civil Engineering, University of Patras, Patras, Greece

Received 15 June 2004; revised 23 May 2005; accepted 6 July 2005; published 25 October 2005.

[1] A field-scale experiment was conducted at a research site using bacterial viruses (bacteriophage) MS2 and PRD1 as surrogates for human viruses, bromide as a conservative tracer, and tertiary-treated municipal wastewater (recycled water) to investigate the fate and transport of viruses during artificial recharge. Observed virus concentrations were fitted using a mathematical model that simulates virus transport in one-dimensional, homogeneous, water-saturated porous media accounting for virus sorption (or filtration), virus inactivation, and time-dependent source concentration. The fitted time-dependent clogging rate constants were used to estimate the collision efficiencies for bacteriophage MS2 and PRD1 during vertical fully saturated flow. Furthermore, the corresponding time-dependent collision efficiencies for both bacteriophage asymptotically reached similar values at the various sampling locations. These results can be used to develop an optimal management scenario to maximize the amount of recycled water that can be applied to the spreading grounds while still maintaining favorable attachment conditions for virus removal.

Citation: Anders, R., and C. V. Chrysikopoulos (2005), Virus fate and transport during artificial recharge with recycled water, *Water Resour. Res.*, *41*, W10415, doi:10.1029/2004WR003419.

1. Introduction

[2] The use of treated municipal wastewater effluent (recycled water) for artificial recharge of groundwater is increasing, especially in the southwestern United States. In many areas artificial recharge is accomplished by delivering large amounts of water, including recycled water, to large holding ponds, or spreading grounds. One concern with using recycled water is that active/infective human enteric viruses might be delivered with the recycled water to the spreading grounds. Therefore retention and inactivation of viruses on the soil during recharge is considered to be the final step in a multibarrier treatment system to protect public health [*National Research Council*, 1994]. In California, the Department of Health Services (DOHS) governs the recharge of groundwater with recycled water. The proposed State of California criteria for artificial recharge with recycled water states that the applied municipal wastewater used for surface spreading should be retained underground for a minimum of 6 months prior to extraction for use as a drinking water supply, and should not be extracted within 500 feet (153 m) of the point of recharge [*Hultquist et al.*, 1991; *Asano and Cotruvo*, 2004]. These provisions were established to protect groundwater resources by ensuring that adequate retention time and distance requirements are met for pathogen removal.

[3] The major processes controlling the subsurface transport of viruses are their sorption characteristics and/or rate of inactivation [*Gerba and Keswick*, 1981]. Inactivation of viruses suspended in the liquid phase as well as viruses sorbed to soil particles is controlled by degradation of the viral capsid and by subsurface temperature [*Yates*, 1987]. The degree of virus sorption during subsurface transport is affected by several factors including viral surface properties, groundwater quality, and sediment surface charges [*Gerba*, 1984]. Several investigators have treated viruses as solutes due to their small size [*Grosser*, 1984; *Tim and Mostaghimi*, 1991; *Park et al.*, 1992; *Vilker and Burge*, 1980; *Sim and Chrysikopoulos*, 1995, 1998, 1999; *Chrysikopoulos and Sim*, 1996], or described the physical and chemical factors that influence their sorption onto the solid matrix by the colloid filtration theory [*Bales et al.*, 1991; *Kinoshita et al.*, 1993; *Sim and Chrysikopoulos*, 1995; *Pieper et al.*, 1997; *Redman et al.*, 1997; *Deborde et al.*, 1999; *Ryan et al.*, 1999; *Schijven et al.*, 1999]. Filtration theory is commonly used to describe the removal of colloidal particles (i.e., viruses) during pack bed filtration in water treatment applications [*Yao et al.*, 1971]. The colloid filtration model assumes that particle attachment is governed by the collision efficiency which represents the ratio of the rate of collisions resulting in attachment to the total number of collisions [*Rajagopalan and Tien*, 1976; *Tufenkji and Elimelech*, 2004]. Although

0043-1397/05/2004WR003419$09.00

reversible sorption and inactivation of viruses in laboratory-scale column experiments are typically negligible due to short residence times [*Tufenkji et al.*, 2003], any attempt to evaluate field-scale virus transport under water saturated flow conditions requires the determination of desorption rate constants as well as inactivation constants of suspended and sorbed viruses [*Schijven et al.*, 2003]. Furthermore, during artificial recharge, the subsurface beneath spreading grounds can exhibit significant changes in water flux and hydraulic conditions over time due to the presence of trapped air, sealing of the soil surface, and the effect of biofilms sealing the pores within the wetted zones [*Faybishenko*, 1995]. Therefore field-scale experiments conducted under actual recharge conditions with recycled water using surrogates for human viruses are needed to obtain the information necessary to establish adequate retention time and distance requirements for pathogen removal.

[4] In the present work, virus concentrations measured during a field-scale recharge experiment were fitted using a newly developed mathematical model that simulates virus transport in one-dimensional, homogeneous, water-saturated porous media accounting for virus sorption (or filtration) and inactivation. The analytical solution is also applicable to the special case of time-dependent source concentration. The fitted clogging and declogging rate constants as well as the inactivation constants of suspended and sorbed viruses were used to estimate the collision efficiency of bacteriophage MS2 and PRD1 during vertical fully water-saturated flow.

2. Site Description

[5] A field-scale recharge experiment was conducted during August through September 1998 at the USGS research field site located in Los Angeles County, California [*Anders et al.*, 2004]. A map of the research site location is shown in Figure 1. The research field site consists of a test basin and adjacent desilting basin at the north end of the San Gabriel River Coastal Basin Spreading Grounds, a large recharge facility (spreading grounds) providing groundwater replenishment to the Montebello Forebay in Los Angeles County. Tertiary-treated effluent from the San Jose Creek Water Reclamation Plant, which has undergone chlorination-dechlorination and either monomedia (anthracite only) or dual-media (anthracite and sand) filtration, is delivered through a 2.4 m diameter culvert to the spreading grounds. A portion of the flow can be diverted on demand to the research site through a 15.2 cm pipeline using a 1,100 m^3/d pump installed in the culvert.

[6] Construction of the test basin exposed an effective percolation area of about 500 m^2 at a maximum operating water depth of about 2.4 m. Instrumentation at the research site used for the recharge experiment included two steel well points located within the center of the test basin installed at depths of about 2.1 and 3.6 m below the surface (WP1 and WP2, respectively). The well points consist of a 0.15 m conical drive shoe at the bottom, 0.6 m screens, and galvanized steel pipe. The steel well points were hydraulically developed by air surging. *Schroeder et al.* [2003] provides additional details of the instrumentation at the research site.

[7] Core material was collected during the construction of the test basin by driving a flame-sterilized, split-spoon core barrel through the bottom of the hole produced by hollow-stem augering. The core material was recovered at approximately 0.3 m intervals to a depth of 10.6 m below the floor of the test basin. A lithology log compiled from field observations and measured grain size distributions indicated that the soil beneath the test basin is predominantly fine (0.125 mm) to coarse (1.0 mm), moderately sorted, grayish-brown sand [*Schroeder et al.*, 2003].

3. Methods

3.1. Field Preparation

[8] Prior to starting the field-scale experiment, the soil surface of the test basin was tilled to breakup any hardpan that might have remained from previous spreading operations. Throughout the experiment, temperature, pH, and specific conductance were periodically measured in order to monitor possible water quality changes in the test basin itself and in the subsurface beneath the test basin. Field measurements of pH and specific conductance were made using portable pH meter (Orion model 250A) with a pH combination electrode (Orion model 9106) and a portable temperature-compensated conductivity meter (Orion model 124), respectively. Water temperatures were measured using a hand-held alcohol-filled thermometer.

[9] The well points were purged prior to water sample collection by removing three casing volumes with a submersible SP-300R sampling pump system (Fultz Pumps, Inc., Lewistown, PA). As soon as the specific conductance, pH, and temperature measurements had stabilized, 0.6 cm PFE-Teflon tubing was inserted into the casing of each well point at depths of 1.5 m (WP1) and 3.0 m (WP2) beneath the floor of the test basin to allow for low-flow ($\sim$200 mL/min) continuous sampling with peristaltic pumps.

3.2. Bromide Analysis

[10] Bromide, in the form of potassium bromide (Ameribrom Inc., New York, NY, photo grade), was chosen as the conservative tracer to track the recharge front and to estimate dilution of the recycled water by soil moisture and/or groundwater during recharge. It should be noted that alkali halides are the most commonly used salts for subsurface fluid tracing [*Chrysikopoulos*, 1993]. All water samples for bromide analysis were collected into 125 mL polyethylene bottles and bromide concentrations were measured at the USGS National Water Quality Laboratory (Denver, CO) using ion chromatography.

3.3. Bacteriophage Assays

[11] The male-specific RNA coliphage, MS2, and the *Salmonella typhimurium* phage, PRD1, bacterial viruses representative of those found in treated municipal wastewater and in recycled water [*Yanko et al.*, 1999], were used as surrogates for human viruses for the field experiment. These bacteriophage have been used extensively in subsurface virus transport studies and are considered to be good model viruses because they behave more conservatively (attach less) than many pathogenic viruses and are relatively persistent during transport through the subsurface [*Bales et al.*, 1997; *Jin et al.*, 1997; *Ryan et al.*, 1999; *Schijven et al.*, 1999]. Water samples for bacteriophage analyzes were collected into sterile bottles and stored at 4°C until the

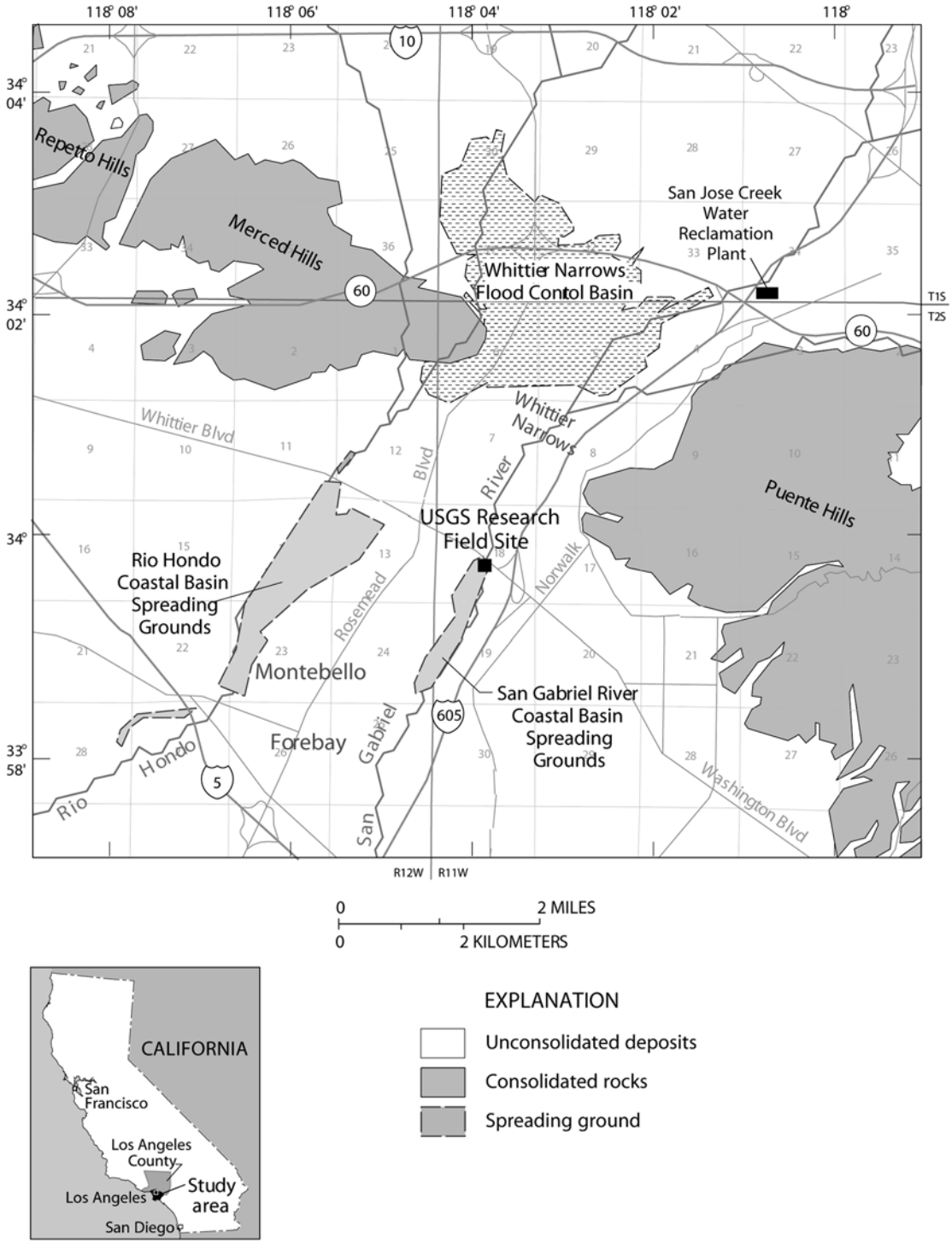

Figure 1. Location of the research field site in Los Angeles County, California.

bacteriophage concentrations were measured at the County Sanitation Districts of Los Angeles County (CSDLAC) virology laboratory.

[12] Bacteriophage concentrations were measured using either the double agar layer assay [*Adams*, 1959] or most probable number (MPN) procedure [*Kott*, 1966]. Trypticase soy broth (TSB) (Difco), TSB (Difco) soft agar (containing 0.05% 1N $CaCl_2$) and TSA (Difco) bottom agar were used for analyzing PRD1 bacteriophage using *Salmonella typhimurium* LT2 (American type culture collection (ATCC) 15277) as the host bacteria, and for analyzing MS2 bacteriophage using *E. coli* F^-amp (ATCC 700891) as the host bacteria with the same concentration of antibiotics as described by *Debartolomeis and Cabelli* [1991]. The double agar layer assay was estimated to have a detection limit of 0.5 plaque-forming units (PFU)/mL, whereas the MPN

method employed in this study was estimated to have a detection limit of 0.02 MPN PFU/mL.

3.4. Tracer Injection

[13] Recycled water was delivered from the culvert to the test basin at a rate of about 1063 m^3/d for several days. Eventually, a mound was established and the test basin began to fill with recycled water. At the start of the experiment, the depth and volume of recycled water in the test basin was about 1.2 m and 473 m^3, respectively. Because direct sunlight may significantly affect the inactivation rates of bacteria and bacteriophage [*Sinton et al.*, 1999], PRD1 and MS2 were introduced into the test basin during the evening or early morning when inactivation from ultraviolet radiation or photolysis would be minimal. The initial seeding was accomplished by spraying the surface of the water in the test basin with solutions containing 8.5×10^{11} PFU of PRD1, 8.5×10^{13} PFU of MS2, and 72.9 kg of potassium bromide (49 kg of Br). After completion of the initial seeding of the test basin, 4.7×10^{12} PFU of PRD1, 6.0×10^{13} PFU of MS2, and 16.4 kg of potassium bromide (11 kg of Br), were injected with peristaltic pumps directly into the feed pipe delivering recycled water to the test basin. After completion of the injection process, the delivery of recycled water to the test basin was halted for 16 hours, and subsequently resumed without addition of bacteriophage and bromide. Water samples were collected at 1.5 and 3.0 m beneath the floor of the test basin (sampling points WP1 and WP2) and from the test basin itself for a period of 9 days.

4. Model Development

[14] One-dimensional virus transport in homogeneous, saturated porous media accounting for virus sorption (or filtration) and inactivation is governed by the following partial differential equation [*Sim and Chrysikopoulos*, 1995]

$$\frac{\partial C(t,z)}{\partial t}+\frac{\rho}{\theta}\frac{\partial C^*(t,z)}{\partial t}=D\frac{\partial^2 C(t,z)}{\partial z^2}-U\frac{\partial C(t,z)}{\partial z}-\lambda C(t,z) - \lambda^*\frac{\rho_b}{\theta}C^*(t,z), \tag{1}$$

where C is the concentration of virus in suspension; C^* is the concentration of virus sorbed on the solid matrix; D is the hydrodynamic dispersion coefficient; U is the average interstitial velocity; ρ_b is the bulk density of the solid matrix; λ is the inactivation rate constant of suspended viruses; λ^* is the inactivation rate constant of sorbed viruses; θ is the porosity of porous medium; t is time; and z is the coordinate in the direction of flow. The left-hand side of (1) consists of the accumulation terms, and the last two terms represent the inactivation of suspended and adsorbed viruses, respectively. The rate of virus attachment onto the solid matrix is described by the following generalized expression

$$\frac{\rho}{\theta}\frac{\partial C^*(t,z)}{\partial t}=r_1 C(t,z)-r_2 C^*(t,z), \tag{2}$$

where r_1 and r_2 are the forward and the reverse rate coefficients.

[15] The desired expression for C^* is obtained by solving (2) subject to an initial condition of zero sorbed (or filtered) virus concentration ($C^*(0, z) = 0$) as

$$C^*(t,z)=\frac{r_1\theta}{\rho_b}\int_0^t C(\tau,z)\exp\left[-\frac{r_2\theta}{\rho_b}(t-\tau)\right]d\tau. \tag{3}$$

In the view of (2) and (3) the governing equation (1) can be written as

$$\frac{\partial C(t,z)}{\partial t}=D\frac{\partial^2 C(t,z)}{\partial z^2}-U\frac{\partial C(t,z)}{\partial z}-\mathcal{A}C(t,z) - \mathcal{B}\int_0^t C(\tau,z)e^{-\mathcal{H}(t-\tau)}d\tau, \tag{4}$$

where the following substitutions have been employed

$$\mathcal{A}=r_1+\lambda, \tag{5}$$

$$\mathcal{B}=r_1(\lambda^*-\mathcal{H}), \tag{6}$$

$$\mathcal{H}=\frac{\theta r_2}{\rho_b}. \tag{7}$$

[16] For a semi-infinite, one-dimensional porous medium in the presence of a broad pulse input of viruses, the appropriate initial and boundary conditions are

$$C(0,z)=0, \tag{8}$$

$$-D\frac{\partial C(t,0)}{\partial z}+UC(t,0)=\begin{cases} UC_0(t) & 0<t\le t_p,\\ 0 & t>t_p,\end{cases} \tag{9}$$

$$\frac{\partial C(t,\infty)}{\partial z}=0, \tag{10}$$

where $C_0(t)$ is the time-dependent source concentration, and t_p is the duration of the solute pulse. The condition (8) establishes that there is no initial virus concentration within the porous medium. The constant flux boundary condition (9) implies virus concentration discontinuity at the inlet and that the source concentration is not constant during the broad pulse. The downstream boundary condition (10) preserves concentration continuity for a semi-infinite system.

[17] An analytical solution to the problem described by the governing partial differential equation (4) subject to initial and boundary conditions (8)–(10) has been derived by *Sim and Chrysikopoulos* [1995] for the case of continuous and time-invariant (constant) source concentration. The *Sim and Chrysikopoulos* [1995] model was modified by *Keller et al.* [2004] to account for the special case of a single, time-invariant broad pulse source concentration. For the general case of a time-dependent broad pulse source concentration described in this study, an analytical solution can be obtained with application of the principle of superposition, as suggested by *Chrysikopoulos et al.* [1990] and

Chrysikopoulos and Lee [1998]. Assuming that the broad pulse t_p consists of several subpulses

$$t_p = t_{p(1)} + t_{p(2)} + \cdots + t_{p(M)}, \tag{11}$$

where $t_{p(m)}$ (m = 1, 2, …, M) represents the time period of subpulse m. For the duration of each subpulse the source concentration, $C_{0(m)}$, is assumed to remain constant. The solution is expressed as

$$C(t,z) = \sum_{m=1}^{M} C_{0(m)}(t)\left[\Phi(t-\hat{t}_{m-1},z) - \Phi(t-\hat{t}_m,z)\right], \quad (t > t_p), \tag{12}$$

where

$$\hat{t}_{m-1} = \sum_{i=1}^{m-1} t_{p(i)}, \tag{13}$$

$$\hat{t}_m = \sum_{i=1}^{m} t_{p(i)}, \tag{14}$$

$$\begin{aligned}\Phi(t,z) = {} & \frac{U}{D^{1/2}}\exp\left[\frac{Uz}{2D}\right]\left\{\int_0^t\int_0^\tau \mathcal{H}e^{-\mathcal{H}\tau}J_0\left[2(\mathcal{B}\zeta(\tau-\zeta))^{1/2}\right]\right. \\ & \times\left\{\frac{1}{(\pi\zeta)^{1/2}}\exp\left[\frac{-z^2}{4D\zeta}+\left(\mathcal{H}-\mathcal{A}-\frac{U^2}{4D}\right)\zeta\right]\right. \\ & -\left.\frac{U}{2D^{1/2}}\exp\left[\frac{Uz}{2D}+(\mathcal{H}-\mathcal{A})\zeta\right]\right. \\ & \times\left.\left.\operatorname{erfc}\left[\frac{z}{2(D\zeta)^{1/2}}+\frac{U}{2}\left(\frac{\zeta}{D}\right)^{1/2}\right]\right\}d\zeta d\tau\right. \\ & +e^{-\mathcal{H}t}\int_0^t J_0\left[2(\mathcal{B}\zeta(t-\zeta))^{1/2}\right] \\ & \times\left\{\frac{1}{(\pi\zeta)^{1/2}}\exp\left[\frac{-z^2}{4D\zeta}+\left(\mathcal{H}-\mathcal{A}-\frac{U^2}{4D}\right)\zeta\right]\right. \\ & -\left.\frac{U}{2D^{1/2}}\exp\left[\frac{Uz}{2D}+(\mathcal{H}-\mathcal{A})\zeta\right]\right. \\ & \times\left.\operatorname{erfc}\left[\frac{z}{2(D\zeta)^{1/2}}+\frac{U}{2}\left(\frac{\zeta}{D}\right)^{1/2}\right]\right\}d\zeta\end{aligned} \tag{15}$$

[18] The Bessel function relationship $I_0(x) = J_0(ix)$, where I_0 is the modified Bessel function of the first kind of zeroth order and x is an arbitrary argument [*Abramowitz and Stegun*, 1972], can be used for the evaluation of $J_0(ix)$ with complex argument. The solution (12) can also be used for early times ($t < t_p$); however, if $\hat{t}_{m-1} < t < \hat{t}_m$ then $\Phi(t - \hat{t}_m) = 0$. It should be noted that for the derivation of (12) the superposition principle can be employed because the governing partial differential equation (1) is linear with respect to the aqueous phase concentration.

[19] For this work, COLLOIDFIT, a program written in FORTRAN, was develop to fit the virus transport model (14) to the experimental data. COLLOIDFIT utilizes subroutine mrqmin [*Press et al.*, 1992] for the nonlinear least squares regression, and subroutines qdag and twodq [*International Mathematics and Statistics Libraries*, 1991] for the numerical evaluation of the single and double integrals, respectively, present in (15).

4.1. Determination of Collision Efficiency

[20] The forward and the reverse rate coefficients presented in (2) are defined as [*Sim and Chrysikopoulos*, 1995]

$$r_1 = k_c = U\phi F(C^*), \tag{16}$$

$$r_2 = \frac{\rho}{\theta}(k_r + \lambda^*), \tag{17}$$

respectively, where k_c is the clogging rate constant, ϕ is the filter coefficient, $F(C^*)$ is the dynamic blocking function that accounts for variations of porosity with increasing particle attachment, and k_r is the declogging rate constant. For the filtration of submicron particles such as viruses, it is assumed that $F(C^*) = 1$ and (16) reduces to

$$k_c = U\phi. \tag{18}$$

The filter coefficient is expressed as [*Rajagopalan and Tien*, 1976]

$$\phi = \frac{3(1-\theta)}{2d_p}\eta, \tag{19}$$

where η is the single collector removal efficiency of the filter and d_p = 0.25 mm is the average grain diameter of the porous medium.

[21] Note that the single collector removal efficiency presented in (19) is commonly expressed as [*Yao et al.*, 1971]

$$\eta = \alpha\eta_0, \tag{20}$$

where α is the collision efficiency, and η_0 is the single collector removal efficiency for favorable deposition (in the absence of double layer interaction energy). Combining (18), (19), and (20) yields the following expression for the collision efficiency factor

$$\alpha = \frac{k_c}{U}\frac{2d_p}{3(1-\theta)}\frac{1}{\eta_0}. \tag{21}$$

[22] An approximate expression for η_0 applicable to deep bed filtration based on the Happel sphere-in-cell porous media model is the following [*Rajagopalan and Tien*, 1976; *Logan et al.*, 1995]:

$$\eta_0 = A_s N_{Lo}^{1/8} N_R^{15/8} + 3.375\times10^{-3} A_s N_G^{1.2} N_R^{-0.4} + 4A_s^{1/3} N_{Pe}^{-2/3}, \tag{22}$$

where A_s is the porosity-dependent flow parameter defined as

$$A_s = \frac{1-\varepsilon^5}{1-1.5\varepsilon+1.5\varepsilon^5-\varepsilon^6}, \tag{23}$$

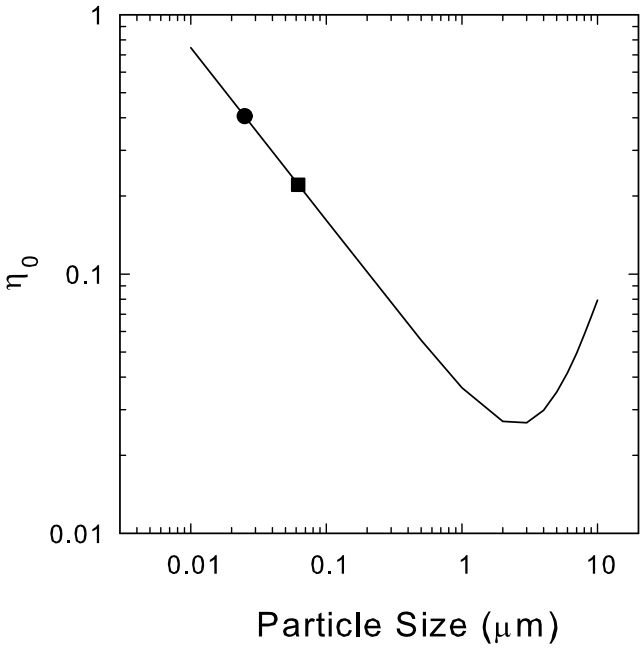

Figure 2. Predicted single collector removal efficiency based on (22) (solid line) and η_0 values for MS2 (circle) and PRD1 (square) for the initial conditions at the field site. Here U = 25.3 cm/hr, d_p = 0.25 mm, θ = 0.3, $H = 6.6 \times 10^{-21}$ (kg m^2)/s^2, $\rho_v \approx \rho_f$, and T = 298 K.

(where $\varepsilon = (1 - \theta)^{1/3}$), N_{Lo} is the London group:

$$N_{Lo} = \frac{4H}{9\pi\mu d_v^2 q}, \tag{24}$$

N_r is the relative size group:

$$N_R = \frac{d_v}{d_p}, \tag{25}$$

N_G is the gravity group:

$$N_G = \frac{d_v^2\left(\rho_v - \rho_f\right)g}{18\mu q}, \tag{26}$$

N_{Pe} is the Peclet number:

$$N_{Pe} = \frac{d_p q}{\mathcal{D}}, \tag{27}$$

where $q = U\theta$ is the specific discharge or the approach velocity, $\mathcal{D}$ is the virus diffusivity governed by Brownian motion and described by the Stokes-Einstein equation as [*Atkins*, 1990]

$$\mathcal{D} = \frac{k_B T}{3\pi\mu d_v}, \tag{28}$$

$k_B = 1.38 \times 10^{-23}$ (kg m^2)/(s^2 K) is the Boltzman constant, $H = 6.6 \times 10^{-21}$ (kg m^2)/s^2 is the Hamaker constant [*Truesdail et al.*, 1998], d_v is the virus diameter (2.5×10^{-8} m for MS2 and 6.2×10^{-8} m for PRD1 [*Kinoshita et al.*, 1993]), ρ_v is the virus density (assumed at near-neutral buoyancy), ρ_f is the density of water, $\mu = 8.91 \times 10^{-4}$ kg/(m s) is the viscosity of water, $g = 9.81$ m/s^2 is the acceleration due to gravity, and T is the absolute temperature in Kelvin. Figure 2 presents the single collector removal efficiency as a function of particle size predicted by (22), together with the η_0 values for MS2 and PRD1 for the initial field conditions.

[23] An alternative method to calculate α has been proposed by *Harvey and Garabedian* [1991]. Hereafter the method will be referred to as HG. The HG method is based on the relative breakthrough (RB), defined as the ratio of the time-integrated mass of each bacteriophage relative to that of the conservative tracer

$$\mathrm{RB} = \int_0^t \frac{C(t)}{C_0}\mathrm{d}t \Big/ \int_0^t \frac{C_T(t)}{C_{T_0}(t)}\mathrm{d}t, \tag{29}$$

where C_T is the tracer concentration, and subscript 0 indicates initial concentrations in the test basin. The RB can be determined from experimental data by numerical integration of the area under the corresponding normalized breakthrough curves (i.e., trapezoid rule). Furthermore, assuming that the bacteriophage and bromide enter the test basin as a dirac input, α is expressed as [*Harvey and Garabedian*, 1991]

$$\alpha = \frac{d_p\left\{[1 - 2(\alpha_L/\ell_z)\ln \mathrm{RB}]^2 - 1\right\}}{6(1-\theta)\eta_0\alpha_L}, \tag{30}$$

where ℓ_z is the distance from the injection point to the sampling point, and α_L is the longitudinal dispersivity defined as [*Nielsen et al.*, 1986]

$$\alpha_L = \frac{D - \mathcal{D}_e}{|U|^\gamma}, \tag{31}$$

where $\mathcal{D}_e = \mathcal{D}/\tau^*$ is the effective molecular diffusion coefficient (where $\tau^* \geq 1$ is the tortuosity coefficient) and γ is an exponent that for relatively homogeneous, water-saturated systems is approximately equal to 1.

5. Field-Scale Experiment

5.1. Water Quality

[24] The initial water temperature in the test basin was 28.8°C and the specific conductance adjusted to 25°C was 1,005 μS/cm. The initial specific conductance at WP1 was 1,010 μS/cm and increased to 1025 μS/cm during the experiment. The initial temperature at WP2 was 28.6°C and the specific conductance 992 μS/cm; both increased slightly during the experiment. The pH measured from water samples collected from beneath the test basin ranged from 7.3 to 7.6 pH units. Overall, the observed fluctuations in temperature, pH, and specific conductance were minimal; this indicates that chemical conditions changed little during the recharge experiment and were similar to those observed during other recharge experiments conducted at

the research field site [*Schroeder et al.*, 2003; *Anders et al.*, 2004].

5.2. Bacteriophage Inactivation

[25] During the initial seeding and subsequent metered injection of bromide and bacteriophage, 24 grab samples were collected from four locations around the perimeter and near the center of the test basin in order to determine the degree of mixing in the ponded water and to establish the initial concentrations. The average concentrations were $2.4 \pm 1.4 \times 10^5$ PFU/mL for MS2, $2.4 \pm 1.1 \times 10^4$ PFU/mL for PRD1, and 107 ± 28.0 mg/L for bromide. The high standard deviations indicate incomplete mixing in the test basin during the first few hours of the experiment. Measured bromide and bacteriophage concentrations in water samples collected from the test basin during the field-scale recharge experiment are shown in Figure 3. The shaded area in Figure 3 represents the 16 hour period when no recycled water, bacteriophage, or bromide were delivered to the test basin. Figure 3a indicates that the bromide concentration remained essentially constant for the 16 hour period after mixing was complete and before dilution occurred as the delivery of new recycled water resumed. However, as shown in Figures 3b and 3c, bacteriophage concentrations decreased during the 16 hour period probably due to inactivation. Assuming that virus inactivation is a first-order process [*Yates et al.*, 1985; *Chrysikopoulos and Vogler*, 2004] expressed as

$$\ln\left[\frac{C(t)}{C_0}\right] = -\lambda t, \tag{32}$$

the rate of bacteriophage inactivation can be determined by linear regression analysis of the observed normalized bacteriophage log concentrations. Figure 4 shows the bacteriophage log concentrations for the 16 hour period and the corresponding linear regression lines. The slope of the solid line, $\lambda = 0.07$ h^{-1} represents the inactivation rate coefficient for MS2 with a coefficient of determination $r^2 = 0.94$, and the slope of the dashed line, $\lambda = 0.02$ h^{-1} represents the inactivation rate coefficient for PRD1 with $r^2 = 0.36$. The slopes indicate that the inactivation rate of MS2 was higher than that of PRD1, as was also reported by *Yahya et al.* [1993]. It should be noted that the estimated inactivation rate coefficients correspond to a water temperature of 28.8°C and are therefore higher than those reported in the literature for groundwater temperatures of 4°C [*Yates et al.*, 1985; *Powelson et al.*, 1990] or 7°C [*Yahya et al.*, 1993]. In addition to temperature, Brownian coagulation of viruses [*Grant*, 1994] and/or microbial activity [*Jansons et al.*, 1989] may also increase the rate of virus inactivation. However, λ values for bacteriophage MS2 and PRD1 evaluated from (32) can provide an estimate of the retention time required for adequate virus removal. For example, the estimated λ value for PRD1 in the test basin suggests that almost 38-log removal of bacteriophage would occur in 6 months. This period is equal to the underground retention time proposed by the State of California for surface spreading of municipal wastewater [*Asano and Cotruvo*, 2004]. It should be noted here that *Sim and Chrysikopoulos* [1995] have proposed that the inactivation rate coefficient should be considered as a time-dependent parameter, and suggested that virus transport data collected in the vicinity of the source of contamination at early times are more reliable for estimation of inactivation rate coefficients. Furthermore, *Chrysikopoulos and Vogler* [2004] have shown that temporally variable inactivation rate coefficients can significantly affect the predicted virus migration in porous media.

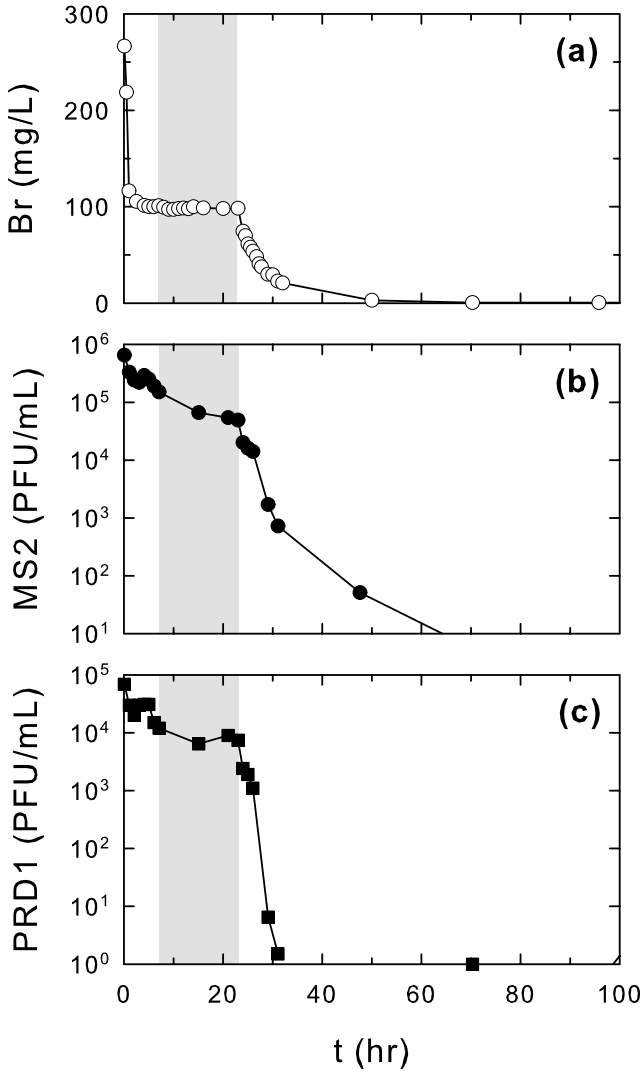

Figure 3. Concentrations of (a) bromide, (b) MS2, and (c) PRD1 in water samples collected from the test basin. Shaded area indicates the 16 hour period when no recycled water was delivered to the test basin.

5.3. Estimation of Transport Parameters

[26] Gauge measurements shown in Figure 5 indicate that the height of recycled water, h, in the test basin remained at about 1.25 m during the initial seeding and injection of bacteriophage and bromide. Furthermore, the shaded area in Figure 5 shows that h decreased from 1.25 m to 0.5 m during the 16 hour period when no recycled water was delivered to the test basin. Once delivery was resumed, h increased to about 1.0 m and remained at that height for the remaining period of the experiment. The recycled water did not return to the original height of 1.25 m due to

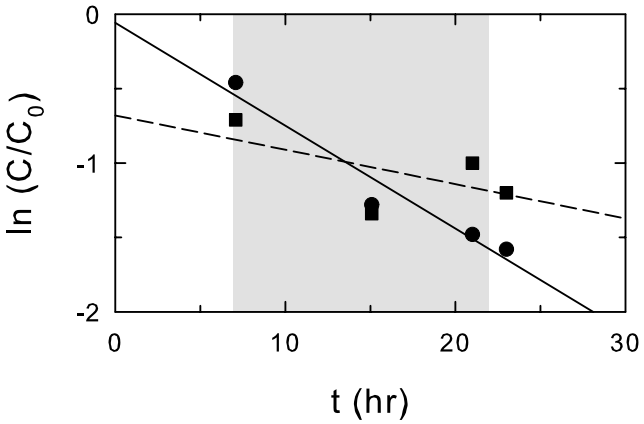

Figure 4. Normalized log concentrations of MS2 (circles) and PRD1 (squares) in the test basin as a function of time. The slope of the fitted lines (solid line for MS2 and dashed line for PRD1) represents the corresponding inactivation rate coefficients. Shaded area represents the 16 hour period when no recycled water was delivered to the test basin.

operations at the spreading grounds that required draining of standing water in the desilting basin adjacent to the test basin.

[27] The bromide concentrations observed at both sampling locations WP1 and WP2 are shown in Figure 6. A comparison of bromide concentrations at WP1 and WP2 to initial concentrations in the test basin indicate that no major dilution occurred at these shallower depths. The mean concentration arrival time for bromide at the sampling locations is defined by the first normalized absolute moment as [*Valocchi*, 1985]

$$m_1 = \int_0^\infty tC_T(t,z)\mathrm{d}t \Big/ \int_0^\infty C_T(t,z)\mathrm{d}t. \qquad (33)$$

First moment analysis of the bromide concentration data provides a mean arrival time of 25.2 hours at WP1 and 28.6 hours at WP2. Also shown in Figure 6 are the model simulated bromide concentration history curves. These curves were constructed with ρ_b = 1.86 gm/cm^3 and θ = 0.3 determined from the measured grain size distribution data and $k_c = k_r = \lambda = \lambda^* = 0$. The parameter values for U and D correspond to the changes in the height of the recycled water in the test basin (vertical gradient) during the field experiment (see Figure 5). Clearly, the absolute minimum number of values for U and D is 4. The parameter values for U and D during the initial seeding and injection of bacteriophage and bromide were fitted by COLLOIDFIT. The remaining U and D values, during the 16 hour period when no recycled water was delivered to the test basin and once delivery was resumed, were calculated from the measured changes in h in the test basin. The broad bromide input pulse was subdivided into 15 subpulses based upon measured bromide concentrations in water samples collected from the test basin during the field-scale recharge experiment (see Figure 3). The time-dependent bromide source concentrations as well as the U and D values for each subpulse at both sampling locations are listed in Table 1. It should be noted that due to the relatively high interstitial velocities, D is governed mainly by mechanical dispersion and the contribution of $\mathcal{D}_e$ is very small. The dispersivity values for the data collected at WP1 and WP2, as determined by (31), are α_L = 1.86 and 1.41 cm, respectively. Note that the estimated dispersivity at WP1 is greater than the one at WP2. Given that the dispersivity is a property of the porous medium, the dispersivity values obtained here indicate that the soil formation beneath the test basin is not perfectly homogeneous. The variation in dispersivity values is relatively small, suggesting that the degree of heterogeneity is slight.

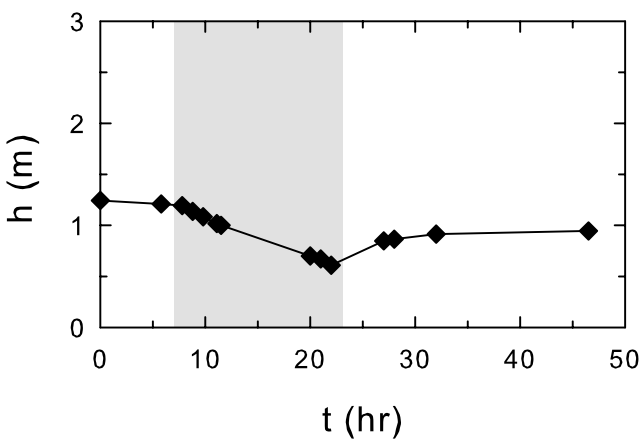

Figure 5. Height of recycled water in the test basin (diamonds) as a function of time. Shaded area represents the 16 hour period when no recycled water was delivered to the test basin.

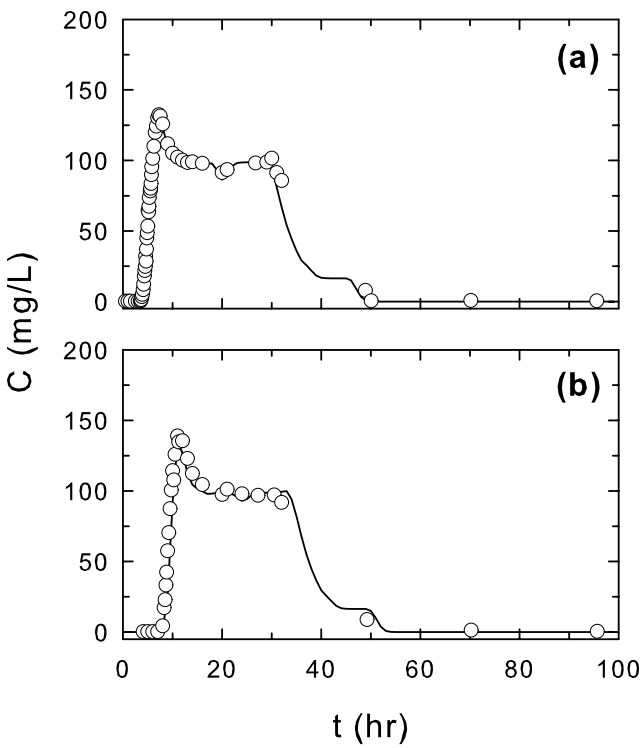

Figure 6. Bromide concentration breakthrough data (circles) observed at (a) WP1 and (b) WP2 and the corresponding simulated concentration histories (curves).

Table 1. Model Parameters for Bromide Breakthrough Data at WP1 and WP2

$t_{p(m)}$, hours	C_{T_0}, mg/L	U, cm/h	D, cm^2/h
	WP1[a]		
0.25	266.5	25.8	48.1
0.75	218.6	25.8	48.1
2.0	116.4	25.8	48.1
4.0	101.1	25.8	48.1
2.0	100.1	25.5	47.5
5.0	98.0	25.5	47.5
8.0	98.7	24.3	45.3
1.0	98.1	24.3	45.3
1.0	98.3	24.7	46.0
1.0	86.4	24.7	46.0
1.0	68.4	24.7	46.0
1.0	57.7	24.7	46.0
2.0	42.0	24.7	46.0
3.0	25.7	24.7	46.0
9.0	16.4	24.7	46.0
	WP2[b]		
0.25	266.5	30.1	42.5
0.75	218.6	30.1	42.5
2.0	116.4	30.1	42.5
4.0	101.1	30.1	42.5
2.0	100.1	29.9	42.2
5.0	98.0	29.9	42.2
8.0	98.0	29.5	41.7
1.0	98.1	29.5	41.7
1.0	98.3	29.7	41.9
1.0	86.4	29.7	41.9
1.0	68.4	29.7	41.9
1.0	57.7	29.7	41.9
2.0	42.0	29.7	41.9
3.0	25.7	29.7	41.9
9.0	16.4	29.7	41.9

[a]For WP1, z = 152.4 cm, and α_L = 1.86 cm.
[b]For WP2, z = 304.8 cm, and α_L = 1.41 cm.

[28] The bacteriophage MS2 concentrations observed at both sampling locations WP1 and WP2 are shown in Figure 6. In contrast to bromide, the first moment of the arrival time for MS2 was 10.3 hours at WP1 and 14.0 hours at WP2. The early mean concentration arrival times of MS2 is attributed to a combination of mechanisms that result in faster velocities and straighter paths [*Sirivithayapakorn and Keller*, 2003]. These mechanisms include pore exclusion, in which the virus particles are excluded from smaller pores based on their size [*Enfield et al.*, 1989; *Abdel-Salam and Chrysikopoulos*, 1995; *Rehmann et al.*, 1999] and/or size exclusion that excludes the virus particles from streamlines near the pore walls [*Ginn*, 2002; *Auset and Keller*, 2004; *Keller et al.*, 2004]. It should be noted that dispersivity can also be a function of colloid size at low Peclet numbers due to the size exclusion effect [*Keller et al.*, 2004].

[29] The bacteriophage MS2 reached a maximum concentration of 6.0×10^4 PFU/mL at WP1 and 3.4×10^4 PFU/mL at WP2. The concentration history curves for MS2 presented in Figure 7 were constructed using U and D values listed in Table 1 and $\lambda = 0.07$ h^{-1} determined from (32). The broad MS2 input pulse was subdivided into 17 subpulses with durations similar to those used for the bromide (see Figure 3). Two subpulses in addition to those employed for the bromide case were required to describe adequately the measured MS2 concentrations during the periods when no recycled water was being delivered to the test basin. Values of k_c for each subpulse were fitted using COLLOIDFIT. All MS2 time-dependent source concentrations as well as the fitted k_c values for each subpulse at both sampling locations are listed in Table 2. Values of k_r and λ^* were fitted using only the receding portion of experimental breakthrough data. Changes in the values of k_r and λ^* affect slightly the slope and intercept of the receding portion of the breakthrough curve, respectively. This observation has also been reported by *Schijven et al.* [1999]. Consequently, these parameters were assumed to remain constant with time but to vary with depth (temporally invariant but spatially variable). The curve in Figure 7a represents the model simulated MS2 breakthrough curve at WP1 with fitted values for $\lambda^* = 0.025$ h^{-1} and $k_r = 5 \times 10^{-4}$ h^{-1}. The initial value of k_c at WP1 was 0.3 h^{-1}; however, when the delivery of recycled water to the test basin was halted, the value of k_c increased to 1.2 h^{-1}. After delivery of recycled water was resumed, k_c values decreased slightly for the remaining period of the experiment. The model simulated MS2 breakthrough curve at WP2 is indicated by the curve in Figure 7b, and it was constructed with fixed value of $\lambda^* = 0.025$ h^{-1} and fitted $k_r = 5 \times 10^{-5}$ h^{-1}. For MS2 at WP2, the initial k_c was 0.2 h^{-1}, this value increased to 0.5 h^{-1} when the delivery of recycled water to the test basin was halted, and then k_c values increased to 0.8 h^{-1} for the remaining period of the experiment. The small fitted values of k_r indicate that desorption does not affect significantly the fate and transport of viruses during vertical fully water-saturated flow.

[30] The bacteriophage PRD1 concentrations observed at both sampling locations WP1 and WP2 are shown in Figure 8. Note that first moment estimated the arrival times

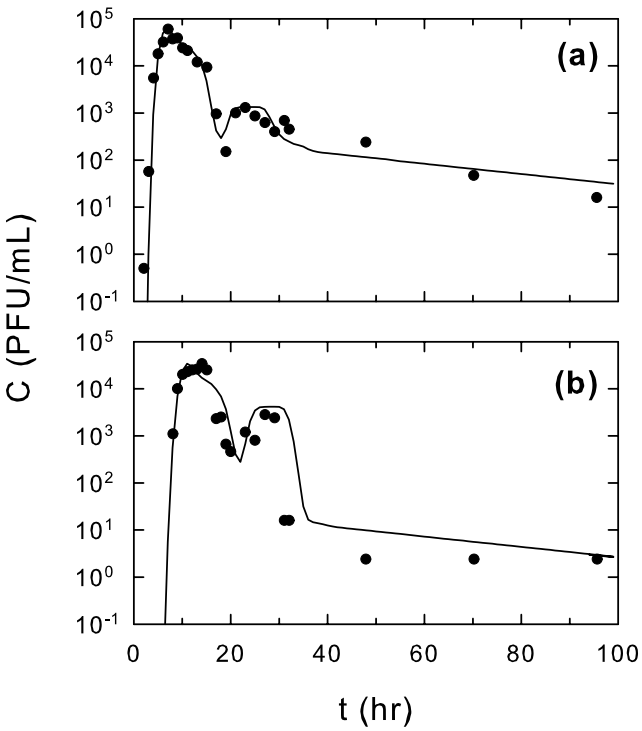

Figure 7. MS2 concentration breakthrough data (circles) observed at (a) WP1 and (b) WP2 and the corresponding simulated concentration histories (curves).

Table 2. Model Parameters for MS2 Breakthrough Data at WP1 and WP2

		k_c, h^{-1}	
$t_{p(m)}$, hours	C_0, PFU/mL	WP1	WP2
2.0	650,000	0.3	0.2
1.0	330,000	0.3	0.2
1.0	260,000	0.3	0.2
1.0	240,000	0.3	0.2
2.0	200,000	0.3	0.2
2.0	110,000	0.3	0.3
5.0	66,000	1.2	0.5
8.0	66,000	0.6	0.2
1.0	54,000	0.8	0.8
1.0	49,000	0.8	0.8
1.0	20,000	0.8	0.8
1.0	16,000	0.8	0.8
1.0	14,000	0.8	0.8
3.0	7,900	0.8	0.8
2.0	1,200	0.8	0.8
16.0	390	0.8	0.8
23.0	2.8	0.8	0.8

for PRD1 at WP1 and WP2 of 10.1 hours and 14.5 hours, respectively, are similar to the arrival times for bacteriophage MS2. Therefore the transport of PRD1 exhibits similar size exclusion behavior as MS2. However, unlike the MS2 data, the peak PRD1 concentration is higher at WP2. The broad PRD1 input pulse was subdivided into the same 17 subpulses used for bacteriophage MS2. All PRD1 time-dependent source concentrations as well as the fitted k_c values for each subpulse at both sampling locations are listed in Table 3. The concentration history curves for PRD1 presented in Figure 8 were constructed following the same procedure described previously for bacteriophage MS2 with $\lambda = 0.02\ h^{-1}$. The model-simulated breakthrough history at WP1 and WP2 presented in Figure 8 by the curves were constructed with $\lambda^* = 0.015\ h^{-1}$ and $k_r = 1 \times 10^{-5}\ h^{-1}$. The values of k_c for PRD1 did not exhibit the same trend as that for MS2, but instead increased slightly at both depths during the recharge experiment and indicate the attachment of PRD1 is affected less by the delivery of recycled water to the test basin. The lack of a similar trend might be explained by noting that the reverse rate coefficient for PRD1 at WP1 and WP2 is $r_2 = 9.35 \times 10^{-2}\ h^{-1}$ which is an order of magnitude less than the forward rate coefficient for most subpulses at both sampling depths.

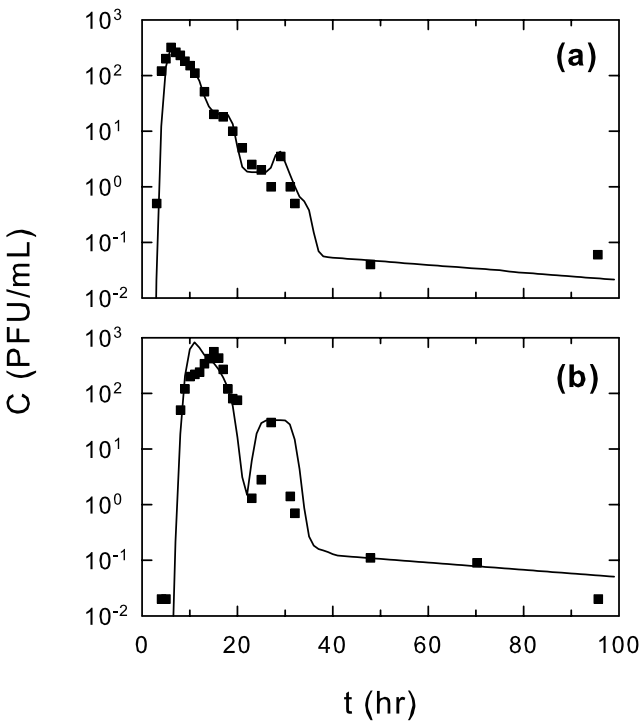

Figure 8. PRD1 concentration breakthrough data (squares) observed at (a) WP1 and (b) WP2 and the corresponding simulated concentration histories (curves).

5.4. Comparison of Collision Efficiencies

[31] Collision efficiencies for both bacteriophage MS2 and PRD1 were estimated with (21) using the fitted time-dependent k_c values and the additional model parameters listed in Table 4. The estimated collision efficiencies suggest more favorable attachment conditions existed for bacteriophage PRD1 than for MS2 during the field-scale recharge experiment. The more favorable attachment conditions (higher collision efficiencies) for bacteriophage PRD1 may be due to its lipid-containing structure and higher hydrophobicity, whereas a more hydrophilic virus such as MS2 behaves more conservatively [*Kinoshita et al.*, 1993]. Figure 9 shows the relationship between k_c and estimated α values for MS2 and PRD1, as well as the corresponding linear regression lines. According to (21) the slope of the lines in Figure 9 is inversely proportional to η_0, and indicates that the soil beneath the test basin is almost twice as efficient at removing PRD1 than MS2 at the conditions present during the experiment. For comparison, the corresponding collision efficiencies were also determined with the HG method and they are listed in Table 5. Figure 10 shows the collision efficiencies as a function of time estimated by both (21) and the HG method. The time-dependent collision efficiencies estimated from the experimentally determined k_c values reached asymptotic values higher than those predicted by the HG method. Note that the

Table 3. Model Parameters for PRD1 Breakthrough Data at WP1 and WP2

		k_c, h^{-1}	
$t_{p(m)}$, hours	C_0, PFU/mL	WP1	WP2
2.0	69,000	0.9	0.4
1.0	30,000	0.9	0.4
1.0	27,000	0.9	0.4
1.0	31,000	0.9	0.4
2.0	19,000	0.9	0.4
2.0	9,200	1.0	0.4
5.0	6,400	1.0	0.9
8.0	6,400	1.4	0.5
1.0	9,000	1.4	1.0
1.0	7,400	1.2	1.0
1.0	2,400	1.2	1.0
1.0	1,900	1.2	1.0
1.0	1,100	1.2	1.0
3.0	550	1.2	1.0
2.0	4.0	1.2	1.0
16.0	1.5	1.2	1.0
23.0	1.0	1.2	1.0

Table 4. Model Parameters for Virus Transport Simulations

Parameter	Value	Units
A_s	75.5	
d_p	2.5×10^{-4}	m
d_v	2.5×10^{-8} (MS2)	m
	6.2×10^{-8} (PRD1)	m
H	6.6×10^{-21}	$(kg\ m^2)/s^2$
k_B	1.38×10^{-23}	$(kg\ m^2)/(s^2\ K)$
T	298	K
ε	0.89	
μ	8.91×10^{-4}	kg/(m s)
ρ_f	999	kg/m^3
ρ_v	1001	kg/m^3

Table 5. Parameters for Estimation of α by the HG Method

	MS2		PRD1	
	WP1	WP2	WP1	WP2
RB	3.35×10^{-2}	1.69×10^{-2}	1.96×10^{-3}	3.43×10^{-3}
η_0	1.59×10^{-1}	1.44×10^{-1}	8.7×10^{-2}	7.86×10^{-2}
α	4.6×10^{-3}	2.7×10^{-3}	1.67×10^{-2}	7.0×10^{-3}

temporal variability of the collision efficiencies cannot be accounted for by the HG method. Furthermore, factors such as temperature and groundwater quality that could affect the degree of attachment have been shown to change very little throughout the duration of the recharge experiment while other factors, such as viral surface properties or sediment surface charge, are not expected to vary greatly during the experiment.

[32] The time-dependent variation in collision efficiencies may in part be attributed to fluctuations in the interstitial fluid velocity caused by changes in recycled water delivery to the test basin. *Veerapaneni and Wiesner* [1997] noted that flow rate influences the morphology of deposits as well as the deposit distribution of monodispersed latex particles filtered through a bed of spherical glass beads. According to *Harter et al.* [2000], a significant decrease in α with decreasing pore velocity indicates either η_0 does not sufficiently describe velocity-dependent filtration phenomena or that chemical interactions between collector and biocolloid (represented by α) are indeed velocity-dependent. *Tufenkji and Elimelech* [2004] developed a new empirical correlation for predicting η_0 that better reflects the significant influence of hydrodynamic interactions on the deposition of microorganisms. However, α values estimated with (21) and (22) are only slightly higher than α values estimated with (21) and the new η_0 empirical relationship developed by *Tufenkji and Elimelech* [2004]. The slight difference indicates the retarding effect of hydrodynamic interactions counterbalances the attractive van der Waals forces experienced by both bacteriophage during the recharge experiment. Furthermore, changes in U affect differently the k_c values for bacteriophage MS2 and PRD1 during the field experiment. Therefore interstitial velocity fluctuations alone cannot adequately explain the α values obtained during this recharge experiment. An alternative explanation is that the estimated time-dependent α values are affected by alterations in the surface structure as well as the porosity of the filtering media during the recharge experiment caused by the presence of entrapped air, sealing of the soil surface, and/or biofilms sealing the pores within the wetted zones.

[33] Collision efficiencies evaluated by the HG method are frequently reported in the literature. *Pieper et al.* [1997] reported that for bacteriophage PRD1 $\alpha = 0.013$ in an uncontaminated aquifer zone and $\alpha = 0.0014$ in a contam-

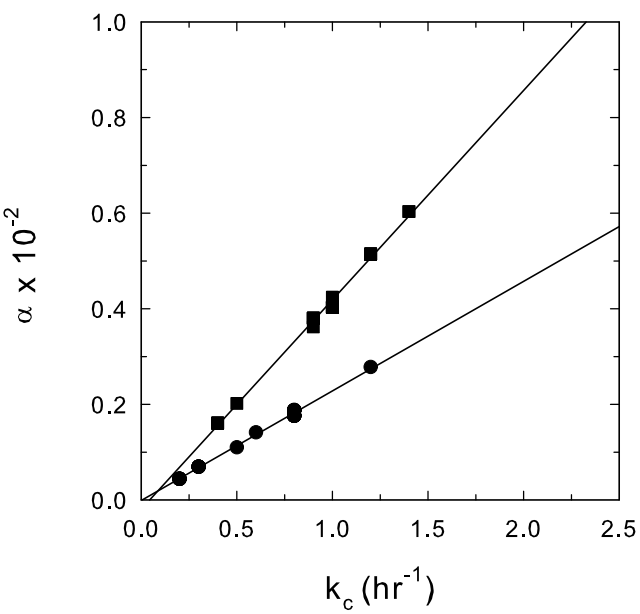

Figure 9. Relationship between k_c and α for MS2 (circles) and PRD1 (squares). Corresponding linear regression lines indicate $\alpha = 2.3 \times 10^{-3} k_c$ for MS2 and $\alpha = 4.4 \times 10^{-3} k_c$ for PRD1.

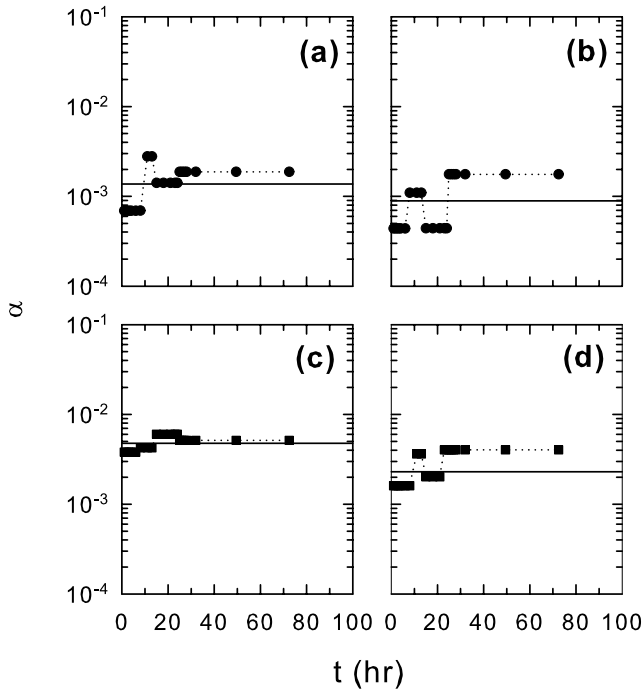

Figure 10. Time-dependent α values for MS2 (circles) at (a) WP1 and (b) WP2 and PRD1 (squares) at (c) WP1 and (d) WP2 together with the corresponding α values estimated by the HG method (solid lines).

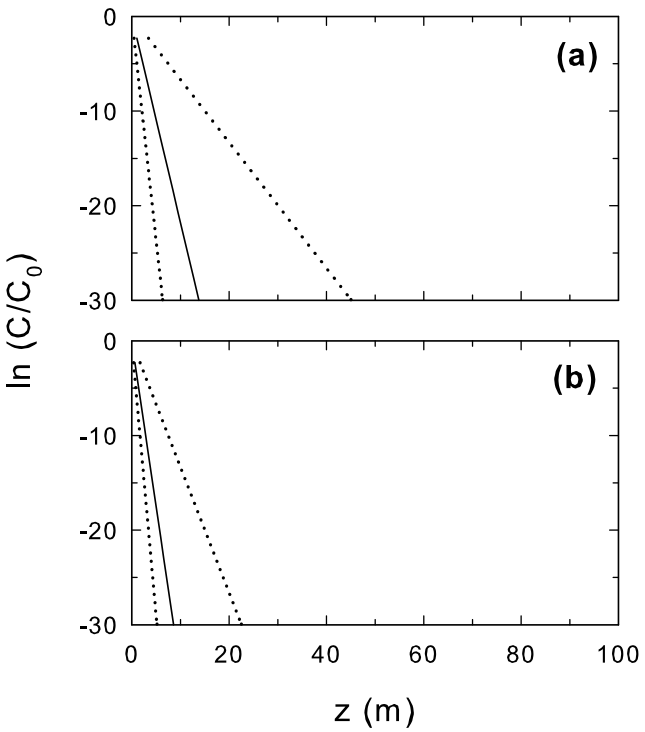

Figure 11. Normalized log concentrations of (a) MS2 and (b) PRD1 in the test basin as a function of distance. The slopes of the solid lines are based on the average ϕ values, and the dotted lines represent the lowest and highest estimated ϕ.

inated zone. The lower collision efficiency (less favorable attachment conditions) in the contaminated zone may be attributed to the presence of dissolved organic matter that enhances bacteriophage transport. *Schroeder et al.* [2003] reported dissolved organic carbon concentrations of almost 10 mg/L in recycled water at the research field site. *Deborde et al.* [1999] calculated that $\alpha = 0.004$ for MS2 and $\alpha = 0.014$ for PRD1 in a gravel-dominated floodplain aquifer. These α values are similar to those obtained in the present study. However, the greater d_p values of 0.00125 m (coarse sand) and 0.012 m (medium pebbles) at that particular field site indicate less favorable attachment conditions existed due to the high groundwater velocities and low specific conductance. *Schijven et al.* [1999] studied the passage of viruses in calcareous, fine dune sand and found that α values ranged from 0.0014 to 0.00027 for MS2 and 0.0024 to 0.00043 for PRD1. These very low α values reflect highly unfavorable conditions for attachment and are consistent with the concept that in sandy soils with relatively high pH values of 7.3–8.3, electrostatic repulsion is important in restricting attachment [*Bales et al.*, 1997]. Considering the slight difference in pH values reported by *Schijven et al.* [1999] and those measured during this experiment, as well as the high velocities during aquifer recharge and the presence of organic matter in recycled water, one would expect less favorable conditions for attachment than those existing in this study.

[34] In view of (18), U and k_c values for each subpulse can be used to obtain the corresponding average experimental ϕ values of 2.18 ± 1.12 m^{-1} ($M = 34$) for MS2 and 3.49 ± 1.32 m^{-1} ($M = 34$) for PRD1 during the field experiment, with the highest values occurring when delivery of recycled water to the test basin was halted. Using the following steady state filtration equation presented by *Logan et al.* [1995] to describe particle removal by isolated spheres

$$\frac{C(t)}{C_0} = \exp\left[-\frac{3(1-\theta)}{2d_p}\eta z\right], \tag{34}$$

and (19), the first-order virus filtration rate is given as

$$\ln\left[\frac{C(t)}{C_0}\right] = -\phi z. \tag{35}$$

It should be noted that ϕ is the summation of individual coefficients representing all physicochemical actions that cause suspended viruses to deposit onto porous media [*Craft and Eichholz*, 1970]. Figure 11 shows a plot of $\ln(C/C_0)$ as a function of z for both MS2 and PRD1. The solid lines in Figure 11 are based on the average of the estimated ϕ values, whereas the dotted lines represent the lowest and highest estimated ϕ values for the conditions of the field recharge experiment. For a desired log removal of viruses, the corresponding z distance represents the appropriate retention distance. For example, using $\phi = 0.66$ m^{-1}, the most conservative ϕ value for MS2 at the conditions of the present study, Figure 11a suggests that over 40-log removal of bacteriophage would occur in 153 m of passage through the subsurface formation. This distance is equal to the separation distance proposed by the State of California for surface spreading of municipal wastewater [*Asano and Cotruvo*, 2004]. Obviously, the λ and ϕ values reported here for bacteriophage MS2 and PRD1 are applicable to the conditions of the specific field site. Results with actual human viral pathogens and different subsurface formations are expected to vary.

6. Summary

[35] Virus concentrations measured during an artificial recharge field-scale experiment were fitted using a newly developed mathematical model that simulates virus transport in one-dimensional homogeneous, water-saturated porous media accounting for virus sorption (or filtration), inactivation, and time-dependent source concentration. The fitted model parameters include the clogging and declogging rate constants, and the inactivation rate constants of suspended and sorbed viruses. These fitted parameters were used to estimate the time-dependent field-scale collision efficiency factors of bacteriophage (MS2 and PRD1). The experimental results of this study can be used for the development of an optimal management scenario that can maximize the amount of recycled water applied to the spreading grounds while still maintaining favorable attachment conditions for virus retention.

Notation

A_s Happel sphere-in-cell model correction factor, defined in (23).

C concentration of virus in suspension, M/L^3.

C^* sorbed virus concentration (virus mass/solid mass), M/M.
C_0 source concentration of virus in suspension, M/L^3.
C_T concentration of bromide, M/L^3.
C_{T_0} source concentration of bromide, M/L^3.
d_p diameter of grain particle, L.
d_v diameter of virus, L.
D hydrodynamic dispersion coefficient, L^2/t.
$\mathcal{D}$ molecular diffusion coefficient, L^2/t.
$\mathcal{D}_e$ effective diffusion coefficient, L^2/t.
g acceleration due to gravity, L/t^2.
h height of recycled water in the test basin, L.
H Hamaker constant, $(M\ L^2)/t^2$.
k_B Boltzman's constant, $(M\ L^2)/(t^2\ K)$.
k_c clogging rate constant, t^{-1}.
k_r declogging rate constant, t^{-1}.
ℓ_z distance between injection and sampling locations, L.
m subpulse number indicator.
m_1 first normalized absolute moment, defined in (33).
M number of subpulses.
N_G gravity group, defined in (26).
N_{Lo} London group, defined in (24).
N_{Pe} Peclet number, defined in (27).
N_R relative size group, defined in (25).
q specific discharge, L/t.
r^2 coefficient of determination.
r_1 forward rate coefficient, t^{-1}.
r_2 reverse rate coefficient, $M/(L^3\ t)$.
t time, t.
t_p duration of the solute pulse, t.
$t_{p(m)}$ time period of a subpulse m, t.
T temperature, in Kelvin.
U average interstitial velocity, L/t.
x spatial coordinate in the horizontal direction, L.
z spatial coordinate in the vertical direction, L.
α collision efficiency.
α_L longitudinal dispersivity, L/t.
γ exponent.
Δt duration of the breakthrough, t.
ε equal to $(1 - \theta)^{1/3}$.
ζ dummy integration variable.
η single collector efficiency.
η_0 single collector efficiency for favorable deposition.
θ porosity of soil (liquid volume/porous medium volume), L^3/L^3.
λ inactivation rate coefficient of suspended bacteriophage, t^{-1}.
λ^* inactivation rate coefficient of adsorbed bacteriophage, t^{-1}.
μ viscosity of the liquid, $M/(L\ t)$.
ρ_b bulk density of the solid matrix (solids mass/aquifer volume), M/L^3.
ρ_f density of the liquid, M/L^3.
ρ_v density of the virus, M/L^3.
τ dummy integration variable.
τ^* tortuosity (≥ 1).
ϕ filter coefficient, L^{-1}.
Φ defined in (19), M/L^3.

[36] **Acknowledgments.** This work was partially sponsored by the CSDLAC, the Water Replenishment District of Southern California, as part of the Soil Aquifer Treatment for Sustainable Water Reuse research program and the Department of Civil and Environmental Engineering at UC Irvine. The authors are grateful to the personnel of the CSDLAC and the USGS for their assistance in conducting the virus tracer experiment.

References

Abdel-Salam, A., and C. V. Chrysikopoulos (1995), Modeling of colloid and colloid-facilitated contaminant transport in a two-dimensional fracture with spatially-variable aperture, *Transp. Porous Media*, *20*, 197–221.

Abramowitz, M., and I. A. Stegun (1972), *Handbook of Mathematical Functions*, 1046 pp., Dover, Mineola, N. Y.

Adams, M. H. (1959), *Bacteriophages*, 592 pp., Wiley-Interscience, Hoboken, N. J.

Anders, R., W. A. Yanko, R. A. Schroeder, and J. L. Jackson (2004), Virus fate and transport during recharge using recycled water at a research field site in the Montebello Forebay, Los Angeles County, California, 1997–2000, *U.S. Geol. Surv. Sci. Invest. Rep., 2004-5161*, 65 pp.

Asano, T., and J. A. Cotruvo (2004), Groundwater recharge with reclaimed municipal wastewater: Health and regulatory considerations, *Water Res.*, *38*, 1941–1951.

Atkins, P. W. (1990), *Physical Chemistry*, 4th ed., 995 pp., Oxford Univ. Press, New York.

Auset, M., and A. A. Keller (2004), Pore-scale processes that control dispersion of colloids in saturated porous media, *Water Resour. Res.*, *40*, W03503, doi:10.1029/2003WR002800.

Bales, R. C., S. R. Hinkle, T. W. Kroeger, K. Stockling, and C. P. Gerba (1991), Bacteriophage adsorption during transport through porous media: Chemical perturbations and reversibility, *Environ. Sci. Technol.*, *25*(12), 2088–2095.

Bales, R. C., S. Li, T. C. J. Yeh, M. E. Lenczewski, and C. P. Gerba (1997), Bacteriophage and microscope transport in saturated porous media: Forced-gradient experiment at Borden, Ontario, *Water Resour. Res.*, *33*, 639–648.

Chrysikopoulos, C. V. (1993), Artificial tracers for geothermal reservoir studies, *Environ. Geol.*, *22*, 60–70.

Chrysikopoulos, C. V., and K. Y. Lee (1998), Contaminant transport resulting from multicomponent nonaqueous phase liquid pool dissolution in three-dimensional subsurface formations, *J. Contam. Hydrol.*, *31*, 1–21.

Chrysikopoulos, C. V., and Y. Sim (1996), One-dimensional virus transport in homogeneous porous media with time-dependent distribution coefficient, *J. Hydrol.*, *185*, 199–219.

Chrysikopoulos, C. V., and E. T. Vogler (2004), Estimation of time dependent virus inactivation rates by geostatistical and resampling techniques: Application to virus transport in porous media, *Stochastic Environ. Res. Risk Assess.*, *18*(2), 67–78.

Chrysikopoulos, C. V., P. V. Roberts, and P. K. Kitanidis (1990), One-dimensional solute transport in porous media with partial well-to-well recirculation: Application to field experiments, *Water Resour. Res.*, *26*, 1189–1195.

Craft, T. F., and G. G. Eichholz (1970), Mechanism of rapid filtration in a uniform filter bed, *Water Resour. Res.*, *6*, 527–537.

Debartolomeis, J., and V. J. Cabelli (1991), Evaluation of an *Escherichia coli* host strain for enumeration of male-specific bacteriophages, *Appl. Environ. Microbiol.*, *57*, 1301–1305.

Deborde, D. C., W. W. Woessner, Q. T. Kiley, and P. Ball (1999), Rapid transport of viruses in a floodplain aquifer, *Water Res.*, *33*(10), 2229–2238.

Enfield, C. G., G. Bengtsson, and R. Lindqvist (1989), Influence of macromolecules on chemical-transport, *Environ. Sci. Technol.*, *23*, 1278–1286.

Faybishenko, B. A. (1995), Hydraulic behavior of quasi-saturated soils in the presence of entrapped air: Laboratory experiments, *Water Resour. Res.*, *31*, 2421–2435.

Gerba, C. P. (1984), Applied and theoretical aspects of virus adsorption to surfaces, *Adv. Appl. Microbiol.*, *30*, 133–168.

Gerba, C. P., and B. H. Keswick (1981), Survival and transport of enteric bacteria and viruses in groundwater, *Stud. Environ. Sci.*, *17*, 511–515.

Ginn, T. R. (2002), A travel time approach to exclusion on transport in porous media, *Water Resour. Res.*, *38*(4), 1041, doi:10.1029/2001WR000865.

Grant, S. B. (1994), Virus coagulation in aqueous environments, *Environ. Sci. Technol.*, *28*, 928–933.

Grosser, P. W. (1984), A one-dimensional mathematical model of virus transport, paper presented at the Second International Conference on Ground-Water Quality Research, Univ. Cent. for Water Res., Okla. State Univ., Tulsa, 26 –29 March .

Harter, T., S. Wagner, and E. R. Atwill (2000), Colloid transport and filtration of *Cryptosporidium parvum* in sandy soils and aquifer sediments, *Environ. Sci. Technol.*, *34*, 62–70.

Harvey, R. W., and S. P. Garabedian (1991), Use of colloid filtration theory in modeling movement of bacteria through a contaminated sandy aquifer, *Environ. Sci. Technol.*, *25*(1), 178–185.

Hultquist, R. H., R. H. Sakaji, and T. Asano (1991), Proposed California regulations for ground water recharge with reclaimed municipal wastewater, paper presented at 1991 Specialty Conference, Environmental Engineering, Am. Soc. of Civ. Eng., Reno, Nev.

International Mathematics and Statistics Libraries (1991), IMSL Math Library user's manual, ver. 2.0, Houston, Tex.

Jansons, J., L. W. Edmonds, B. Speight, and M. R. Bucens (1989), Survival of viruses in groundwater, *Wat. Res.*, *23*, 301–306.

Jin, Y., M. V. Yates, S. S. Thompson, and W. A. Jury (1997), Sorption of viruses during flow through saturated sand columns, *Environ. Sci. Technol.*, *31*(2), 548–555.

Keller, A. A., S. Sirivithayapakorn, and C. V. Chrysikopoulos (2004), Early breakthrough of colloids and bacteriophage MS2 in a water-saturated sand column, *Water Resour. Res.*, *40*, W08304, doi:10.1029/2003WR002676.

Kinoshita, T., R. C. Bales, K. M. Maguire, and C. P. Gerba (1993), Effect of pH on bacteriophage transport through sandy soils, *J. Contam. Hydrol.*, *14*, 55–70.

Kott, Y. (1966), Estimation of low numbers of *Escherichia coli* bacteriophage by use of the most probable number method, *Appl. Environ. Microbiol.*, *14*, 141.

Logan, B. E., D. G. Jewitt, R. G. Arnold, E. J. Bouwer, and C. R. O'Melia (1995), Clarification of clean-bed filtration models, *J. Environ. Eng.*, *121*, 869–873.

National Research Council (1994), *Ground Water Recharge Using Waters of Impaired Quality*, Natl. Acad. Press, Washington, D. C.

Nielsen, D. R., M. T. van Genuchten, and J. W. Biggar (1986), Water flow and solute transport processes in the unsaturated zone, *Water Resour. Res.*, *22*, 89S–108S.

Park, N.-S., T. N. Blanford, and P. S. Huyakorn (1992), VIRALT: A modular semi-analytical and numerical model for simulating viral transport in ground water, report, Int. Ground Water Model. Cent., Colo. Sch. of Mines, Golden.

Pieper, A. P., J. N. Ryan, R. L. Amy, T. H. Illangasekare, and D. W. Metge (1997), Transport and recovery of bacteriophage PRD1 in a sand and gravel aquifer: Effect of sewage-derived organic matter, *Environ. Sci. Technol.*, *31*, 1163–1170.

Powelson, D. K., J. R. Simpson, and C. P. Gerba (1990), Virus transport and survival in saturated and unsaturated flow through soil columns, *J. Environ. Qual.*, *19*, 396–401.

Press, W. H., S. A. Teukolsky, W. T. Vetterling, and B. P. Flannery (1992), *Numerical Recipes in Fortran 77: The Art of Scientific Computing*, 931 pp., Cambridge Univ. Press, New York.

Rajagopalan, R., and C. Tien (1976), Trajectory analysis of deep-bed filtration with the sphere-in-cell porous media model, *AIChE J.*, *22*, 523–533.

Redman, J. A., S. B. Grant, T. M. Olson, M. E. Hardy, and M. K. Estes (1997), Filtration of recombinant Norwalk virus particles and bacteriophage MS2 in quartz sand: Importance of electrostatic interactions, *Environ. Sci. Technol.*, *31*, 3378–3383.

Rehmann, L. L. C., C. Welty, and R. W. Harvey (1999), Stochastic analysis of virus transport in aquifers, *Water Resour. Res.*, *35*, 1987–2006.

Ryan, J. N., E. Elimelech, R. A. Ard, R. W. Harvey, and P. R. Johnson (1999), Bacteriophage PRD1 and silica colloid transport and recovery in an iron oxide-coated sand aquifer, *Environ. Sci. Technol.*, *33*, 63–73.

Schijven, J. F., W. Hoogenboezem, S. M. Hassanizadeh, and J. H. Peters (1999), Modeling removal of bacteriophages MS2 and PRD1 by dune recharge at Castricum, Netherlands, *Water Resour. Res.*, *35*, 1101–1111.

Schijven, J. F., H. A. M. de Bruin, S. M. Hassanizadeh, and A. M. de Roda Husman (2003), Bacteriophage and clostridium spores as indicator organisms for removal of pathogens by passage through saturated dune sand, *Water Res.*, *37*, 2186–2194.

Schroeder, R. A., R. Anders, L. B. Barber, J. A. Leenheer, T. I. Noyes, R. T. Rathbun, K. A. Thorn, and S. J. Younger (2003), Water-quality changes and organic-carbon characterization during recharge with recycled water at a recharge basin in Montebello Forebay, Los Angeles County, California, 1991–1996, *U.S. Geol. Surv. Water Resour. Invest. Rep., 03–3146*, 260 pp.

Sim, Y., and C. V. Chrysikopoulos (1995), Analytical models for one-dimensional virus transport in saturated porous media, *Water Resour. Res.*, *31*, 1429–1437, (Correction, *Water Resour. Res.*, *32*, 1473, 1996.)

Sim, Y., and C. V. Chrysikopoulos (1998), Three-dimensional analytical models for virus transport in saturated porous media, *Transp. Porous Media*, *30*, 87–112.

Sim, Y., and C. V. Chrysikopoulos (1999), Analytical models for virus adsorption and inactivation in unsaturated porous media, *Colloids Surf. A*, *155*, 189–197.

Sinton, L. W., R. K. Finlay, and P. A. Lynch (1999), Sunlight inactivation of fecal bacteriophage and bacteria in sewage-polluted seawater, *Appl. Environ. Microbiol.*, *65*, 3605–3613.

Sirivithayapakorn, S., and A. Keller (2003), Transport of colloids in saturated porous media: A pore-scale observation of the size exclusion effect and colloid acceleration, *Water Resour. Res.*, *39*(4), 1109, doi:10.1029/2002WR001583.

Tim, U. S., and S. Mostaghimi (1991), Model for predicting virus movement through soils, *Ground Water*, *29*, 251–259.

Truesdail, S. E., J. Lukasik, S. R. Farrah, D. O. Shah, and R. B. Dickinson (1998), Analysis of bacterial deposition on metal (Hydr) oxide-coated sand filter media, *J. Colloid Interface Sci.*, *203*(2), 369–378.

Tufenkji, N., and M. Elimelech (2004), Correlation equation for predicting single-collector efficiency in physicochemical filtration in saturated porous media, *Environ. Sci. Technol.*, *38*, 529–536.

Tufenkji, N., J. A. Redman, and M. Elimelech (2003), Interpreting deposition patterns of microbial particles in laboratory-scale column experiments, *Environ. Sci. Technol.*, *37*, 616–623.

Valocchi, A. J. (1985), Validity of the local equilibrium assumption for modeling sorbing solute transport through homogeneous soils, *Water Resour. Res.*, *21*, 808–820.

Veerapaneni, S., and M. R. Wiesner (1997), Deposit morphology and head loss development in porous media, *Environ. Sci. Technol.*, *31*, 2738–2744.

Vilker, V. L., and W. D. Burge (1980), Adsorption mass transfer model for virus transfer in soils, *Water Res.*, *14*, 783–790.

Yahya, M. T., L. Galsomies, C. P. Gerba, and R. C. Bales (1993), Survival of bacteriophage MS-2 and PRD-1 in ground water, *Water Sci. Technol.*, *27*, 409–412.

Yanko, W. A., J. L. Jackson, F. P. Williams, A. S. Walker, and M. S. Castillo (1999), An unexpected temporal pattern of coliphage isolation in groundwaters sampled from wells at varied distances from reclaimed water recharge sites, *Water Res.*, *33*, 53–64.

Yao, K. M., M. T. Habibian, and C. R. O'Melia (1971), Water and waste water filtration: Concepts and applications, *Environ. Sci. Technol.*, *5*, 1105–1112.

Yates, M. V. (1987), Modeling virus survival and transport in the subsurface, *J. Contam. Hydrol.*, *1*, 329–345.

Yates, M. V., C. P. Gerba, and L. M. Kelly (1985), Virus persistence in groundwater, *Appl. Environ. Microbiol.*, *49*, 778–781.

R. Anders, U.S. Geological Survey, 5735 Kearny Villa Road, Suite O, San Diego, CA 92123, USA. (randers@usgs.gov)

C. V. Chrysikopoulos, Department of Civil and Environmental Engineering, University of California, Irvine, CA 92697, USA. (costas@eng.uci.edu)